

Communication

# An Enzyme Cascade Synthesis of Vanillin

Tobias Klaus, Alexander Seifert, Tim Häbe, Bettina M. Nestl and Bernhard Hauer \* 

Institute of Biochemistry and Technical Biochemistry, Department of Technical Biochemistry, Universitaet Stuttgart, Allmandring 31, 70569 Stuttgart, Germany; tobias.klaus@curevac.com (T.K.); alexander.seifert@gmx.net (A.S.); tim.t.haebe@ernaehrung.uni-giessen.de (T.H.); bettina.nestl@itb.uni-stuttgart.de (B.M.N.)

\* Correspondence: bernhard.hauer@itb.uni-stuttgart.de; Tel.: +49-711-685-64523

Received: 30 January 2019; Accepted: 21 February 2019; Published: 12 March 2019



**Abstract:** A novel approach for the synthesis of vanillin employing a three-step two-enzymatic cascade sequence is reported. Cytochrome P450 monooxygenases are known to catalyse the selective hydroxylation of aromatic compounds, which is one of the most challenging chemical reactions. A set of rationally designed variants of CYP102A1 (P450 BM3) from *Bacillus megaterium* at the amino acid positions 47, 51, 87, 328 and 437 was screened for conversion of the substrate 3-methylanisole to vanillyl alcohol via the intermediate product 4-methylguaiaicol. Furthermore, a vanillyl alcohol oxidase (VAO) variant (F454Y) was selected as an alternative enzyme for the transformation of one of the intermediate compounds via vanillyl alcohol to vanillin. As a proof of concept, the bi-enzymatic three-step cascade conversion of 3-methylanisole to vanillin was successfully evaluated both in vitro and in vivo.

**Keywords:** cytochrome P450; vanillin; enzyme cascade; vanillyl alcohol oxidase; flavor compound

## 1. Introduction

Vanillin is one of the most widely used flavouring compounds worldwide. Besides being a flavour ingredient for food and beverages, it is used as a fragrance ingredient in perfumes and cosmetics [1], as well as an intermediate in the chemical and pharmaceutical industries for the production of antifoaming agents, herbicides and drugs [2]. However, natural vanillin extracted from vanilla pods is very expensive, and the chemical synthesis of vanillin has several disadvantages including the lack of substrate selectivity. Therefore, a variety of biotechnological approaches was developed for the production of vanillin from eugenol, isoeugenol, ferulic acid, lignin, glucose, phenolic stilbene, vanillic acid or aromatic amino acid starting materials from renewable feedstocks [3–5].

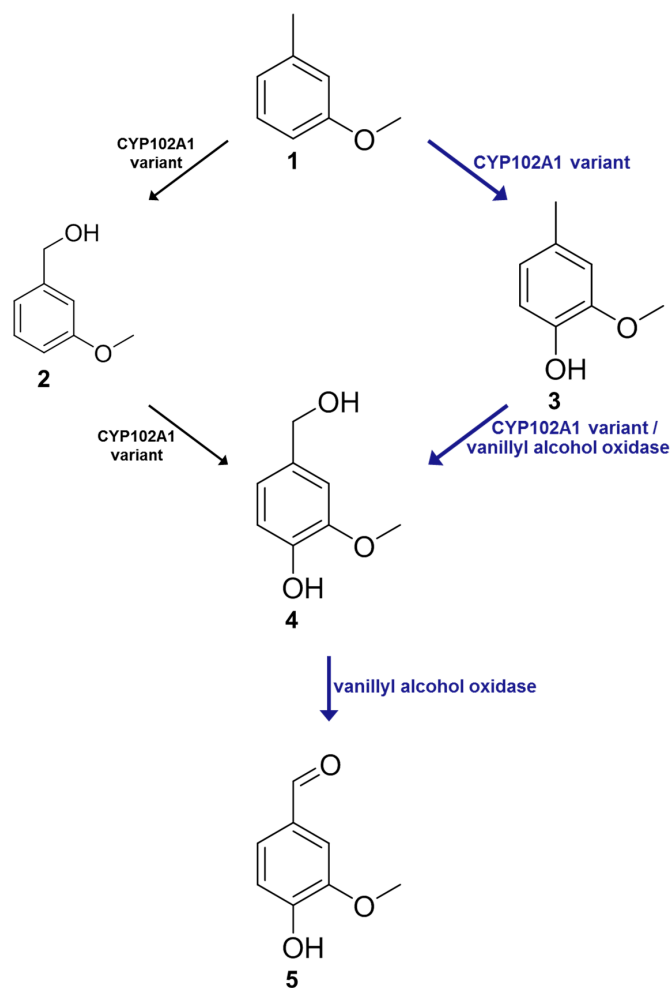
The biotechnological synthesis of vanillin from ferulic acid has gained increasing attention in recent years. Artificial cascades combining a decarboxylase with an oxygenase were developed for the one-pot synthesis of vanillin [6,7]. Aiming at the enzymatic synthesis of vanillin by the selective hydroxylation of an aromatic substrate, cytochrome P450 monooxygenases (P450s) constitute ideal candidates [8]. In general, P450s catalyse oxidation reactions introducing a single oxygen-atom from molecular oxygen into the substrate with the concomitant reduction of the other oxygen atom to water [9]. The electrons necessary for P450-catalysed reactions are usually provided by NAD(P)H and transferred via flavoprotein and/or iron–sulphur redox partner proteins. Recently, these haem-containing proteins have been engineered for non-natural chemistries, thus expanding the biocatalytic repertoire [10–12].

One of the most investigated cytochrome P450 monooxygenases is CYP102A1 (P450 BM3) from *Bacillus megaterium*. It is a natural self-sufficient fusion protein, consisting of a monooxygenase and a diflavin reductase domain [13]. Originally, the wild-type enzyme was found to be a medium- to long-chain fatty-acid hydroxylase, which requires only NADPH and oxygen to function and

hydroxylates exclusively at sub-terminal positions [14]. In the last years, the substrate profile of CYP102A1 has been extended by directed evolution and rational protein design approaches [15–22]. In previous work, a minimal and highly enriched mutant library of CYP102A1 has been constructed by the combination of five hydrophobic amino acids (Ala, Leu, Ile, Phe and Val) at the two positions 87 and 328. These amino acid positions have been identified as hotspots of selectivity and specificity [23], as they are located directly above the haem group and thus are expected to influence the accessibility of the activated haem oxygen from opposite sides of the haem access channel [24]. Both positions were already addressed in numerous previous studies [25]. The focused library, consisting of the CYP102A1 wild-type and 24 variants, was screened for conversion of the terpene substrates (4R)-limonene, nerylacetone, geranylacetone and (+)-valencene. Eleven variants were found, that converted at least one of the substrates with improved regio- or stereoselectivity [24]. Furthermore, variants of CYP102A1 were successfully applied to screen for hydroxylation of cyclic and acyclic alkanes as well as aromatic substrates [21,26,27].

The vanillyl alcohol oxidase (VAO) from *Penicillium simplicissimum* provides an alternative to CYP102A1 and its variants. Similar to eugenol oxidase that has been reported for the synthesis of vanillin from vanillyl alcohol [28], VAO is a flavoprotein with a covalently bound FAD cofactor [29]. It is known to be active with a wide range of 4-hydroxybenzylic compounds [30] and for its catalytic cycle with 4-alkylphenols [31]. Both 4-methylguaiacol and vanillyl alcohol are known to be substrates for VAO [32]. In 2004, van den Heuvel and coworkers identified several single variants of VAO in a random mutagenesis approach, aiming at the generation of an enhanced reactivity concerning the conversion of 4-methylguaiacol to vanillin, showing up to 40-fold increase in catalytic efficiency ( $k_{cat}/K_m$ ) compared with the wild-type enzyme [33].

In the present work, we introduce the concept of enzymatic cascade reactions as an effective means to selectively oxidise aromatic compounds for the synthesis of vanillin from the simple aromatic phenylalkane 3-methylanisole (Scheme 1). In recent years, a plethora of reviews covering multi- and chemo-enzymatic cascades for the production of various natural and non-natural products have been reported [34–43]. By simultaneously screening the minimal and highly enriched CYP102A1 mutant library and by generating CYP102A1 and VAO variants by rational protein design, an alternative system for the synthesis of vanillin was formed as demonstrated by first in vitro and then in vivo transformations.



**Scheme 1.** Proposed reaction pathway for the oxidation of 3-methylanisole (1) to vanillin (5) via the intermediate products 3-methoxybenzyl alcohol (2) or 4-methylguaiacol (3) and vanillyl alcohol (4). The reaction steps are intended to be catalysed by a combination of variants of the cytochrome P450 monooxygenase CYP102A1 and vanillyl alcohol oxidase. The preferred route is highlighted in blue.

## 2. Results and Discussion

### 2.1. Screening of the Small Focused CYP102A1 Library

We studied the P450 enzyme CYP102A1 for the synthesis of vanillin from an aromatic compound in an enzyme-catalysed cascade reaction, as both wild-type and variants of CYP102A1 were previously shown to successfully convert various aromatic substrates [21,25]. Hence, we tested the focused library of CYP102A1 consisting of the wild-type and 24 variants (single and double variants constructed by the combination of five hydrophobic amino acids Ala, Leu, Ile, Phe and Val in two positions 87 and 328). The library was screened for conversion of the substrate 3-methylanisole (1) as well as the intermediate products 3-methoxybenzyl alcohol (2) and 4-methylguaiacol (3) by HPLC. Substrate concentrations of 0.5 mM were used in the first screening. To investigate a possible overoxidation of the intended product vanillyl alcohol (4), this compound was also applied for the screening. Whilst 3-methoxybenzyl alcohol (2), 4-methylguaiacol (3) and vanillyl alcohol (4) were not converted with any of the CYP102A1 variants, conversion of 3-methylanisole (1) was detected with the wild-type as well as 22 of the variants (Table S1). Only two variants displayed no activity towards 3-methylanisole (1) and six variants, including the wild-type, showed only low activity (less than 5% conversion). However, for six variants, a conversion of 3-methylanisole (1) higher than 25% was detected, with five of them having a substitution of phenylalanine at position 87 by valine (F87V). Subsequently, a focus was set

on the variants with the highest conversion results for 3-methylanisole (1), namely the single variants A328L and F87V and the four double variants F87V/A328F/I/L/V. These variants, including the wild-type for comparison, were investigated in more detail by GC–FID for the exact determination of the conversion of substrate 3-methylanisole (1) and the respective product yields (Table 1 and Table S2). Unfortunately, all of the investigated variants with relatively high activity displayed only low selectivity. In addition to the desired intermediate products 3-methoxybenzyl alcohol (2) and 4-methylguaiacol (3), generated by benzylic or aromatic hydroxylation, respectively, four other byproducts could be detected: 4-methoxy-2-methylphenol (6), 2-methoxy-6-methylphenol (8), *m*-cresol (9) and methylhydroquinone (10) (Figure 1). Little product formation of 2-methoxy-6-methylphenol (8) (less than 1%) was detected only using CYP102A1 variants F87V and F87V/A328F (data not shown in Table 1).

Whilst the CYP102A1 wild-type enzyme showed only very low conversion (<1%) of 3-methylanisole (1) with compound 4-methoxy-2-methylphenol (6) as sole product, all single and double variants were much more active towards the substrate. The main product for all reactions was 4-methoxy-2-methylphenol (6), except for the variant F87V/A328L, where a mixture of 3-methoxybenzyl alcohol (2), 4-methoxy-2-methylphenol (6), and *m*-cresol (9) was produced in comparable amounts. The highest activity of about 59% was achieved with F87V/A328L, whereas the respective single variants F87V and A328L displayed only about 15% and 31% total conversion, respectively. Moreover, with F87V/A328L the product yields of 3-methoxybenzyl alcohol (2) and *m*-cresol (9) raised to a maximum and methylhydroquinone (10) came up as a new product. Biotransformations with *m*-cresol (9) and 4-methoxy-2-methylphenol (6) demonstrated that the formation of methylhydroquinone (10) resulted from the conversion of *m*-cresol (9). No product formation of methylhydroquinone (10) was observed in the transformation of 4-methoxy-2-methylphenol (6). While F87V/A328L showed the highest conversion of 3-methylanisole (1) to intermediate product 3-methoxybenzyl alcohol (2) (9.1%), the highest production of 4-methylguaiacol (3) was achieved with the single variant A328L (2.7%). Formation of byproduct 7 was not detected. Overoxidation was detected only for F87V/A328L and F87V/A328V. Methylhydroquinone (10) was identified not to be the product of *O*-demethylation of 4-methoxy-2-methylphenol (6) but to be the product of aromatic hydroxylation of *m*-cresol (9) (data not shown). We assume that the rate-enhancing effect and the site-directing influence by the methyl and methoxy substituents lead to a preference for the aromatic hydroxylation in *ortho* and *para* position of the methyl group (4-methylguaiacol (3), 4-methoxy-2-methylphenol (6), and 2-methoxy-6-methylphenol (8)) and in *para* position of the methoxy group (4-methoxy-2-methylphenol (6)). As a result, 4-methoxy-2-methylphenol (6) was the main product of the conversion of 3-methylanisole (1). Aromatic hydroxylation in *meta* position giving intermediate 3-methoxy-2-methylphenol (7) was clearly not the favoured reaction (Figure 1).

**Table 1.** Selected results of the conversion of 3-methylanisole (1) with variants of CYP102A1. Results for all investigated variants of CYP102A1 are shown in Table S2.

CYP102A1 Variant	Product Yield (% of Initial Substrate)					Total Conversion (%)
	2	3	6	9	10	
wild-type	–	–	<1	–	–	<1
A328L	<1	2.7 ± 0.2	26.6 ± 2.5	<1	–	31.0 ± 2.8
F87V	<1	<1	12.5 ± 0.2	<1	–	14.9 ± 0.3
F87V/A328L	9.1 ± 0.2	1.6 ± 0.1	23.2 ± 0.4	12.0 ± 0.8	13.5 ± 0.8	59.3 ± 1.8
F87V/A328L/L437I	20.0 ± 0.9	<1	14.0 ± 0.7	7.4 ± 1.3	19.3 ± 0.5	61.3 ± 2.9
R47L/Y51F	<1	–	1.5 ± 0.1	–	–	1.6 ± 0.1
R47L/Y51F/F87V/A328V	5.0 ± 0.3	<1	24.0 ± 0.8	3.0 ± 0.1	2.1 ± 0.2	34.9 ± 1.4
R47L/Y51F/F87V/A328L/L437I	13.5 ± 0.4	<1	10.1 ± 0.5	7.7 ± 0.2	17.8 ± 0.8	50.4 ± 1.8

–, not detected or <0.05%; 2, 3-methoxybenzyl alcohol; 3, 4-methylguaiacol; 6, 4-methoxy-2-methylphenol; 9, *m*-cresol; 10, methylhydroquinone. Negative controls showed no conversion. Reactions were performed in triplicates using a volume of 1 mL in Tris–HCl buffer pH 7.5 (50 mM) containing a glucose-6-phosphate (5 mM)/glucose-6-phosphate dehydrogenase (5 U/mL and 1 mM MgCl<sub>2</sub>) cofactor regeneration system. Substrate was added at a final concentration of 0.5 mM from a 25 mM stock solution in dimethyl sulphoxide (DMSO). CYP102A1 and variants thereof were used at a final concentration of 1 μM. Reactions were run at 30 °C and 180 rpm for 2 h. Samples were derivatised and analysed by GC–FID.

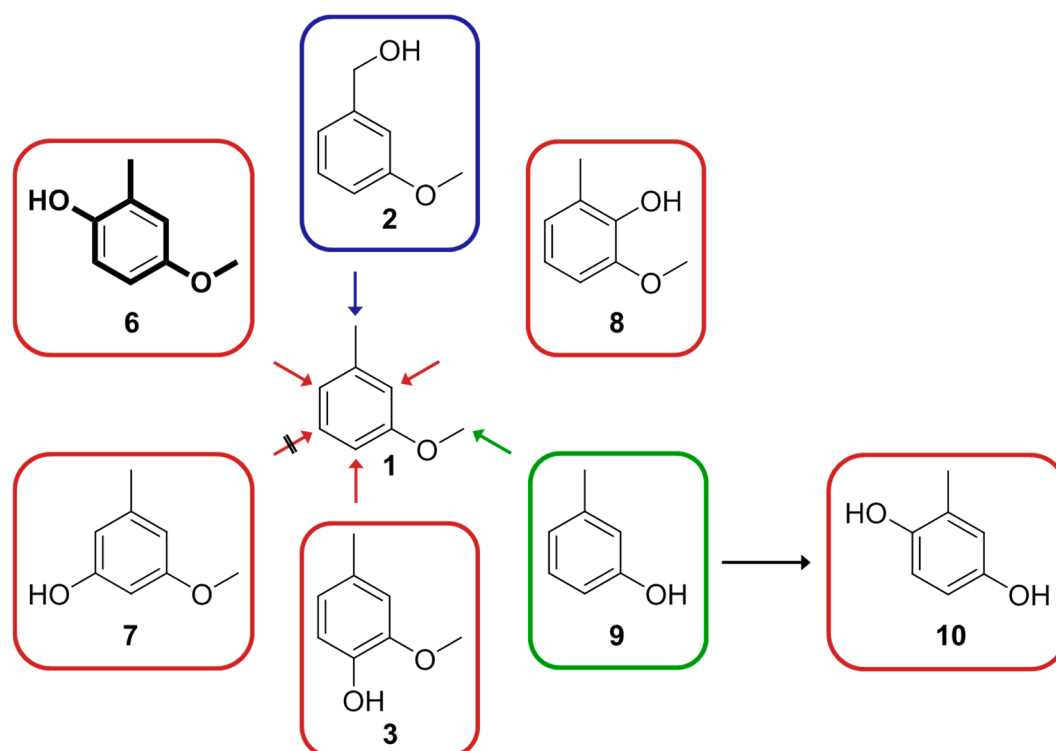


**Figure 1.** Products of the conversion of 3-methylanisole (**1**) with selected CYP102A1 variants. The three potential reaction pathways for vanillin synthesis comprise (indicated with colored arrows; respective reaction product is framed): benzylic hydroxylation (blue), aromatic hydroxylation (red) and O-demethylation (green). Formation of compound 3-methoxy-2-methylphenol (**7**) was not detected. Main product 4-methoxy-2-methylphenol (**6**) is highlighted in bold.

In this work, we have identified that single and double variants displayed a much higher substrate conversion compared to the wild-type, especially those having a valine instead of a phenylalanine at position 87. We assume that this is due to the smaller size of the side-chain of valine compared to phenylalanine, thus allowing a better access and positioning of the substrate to the activated haem oxygen in the active site. This effect of the F87V mutation on the hydroxylation of aromatic compounds, resulting in an improved NADPH-consumption rate and coupling efficiency, was described in a previous work [44]. Unfortunately, the regio- and chemoselectivity of the most active variants was rather low as a variety of oxidation and demethylation products could be detected. Oxidation of the aromatic ring occurred in three of the four possible positions with a preference for the *para* position to the methoxy group, yielding 4-methoxy-2-methylphenol (**6**) as main product. *Meta* hydroxylation did not occur in this work, which is in agreement with the results of a recent study [45].

## 2.2. Screening of Additional CYP102A1 Variants

As the activity concerning the conversion of 3-methylanisole (**1**) could be strongly enhanced by generation of double variants of CYP102A1, additional CYP102A1 variants (triple variants) were investigated with the aim to further improve the enzyme's activity and especially selectivity. In a previous work, it was shown that in addition to the amino acids at positions 87 and 328, the amino acid at position 437 (leucine in the CYP102A1 wild-type) affects the orientation of the substrate to the activated haem oxygen in the active site (Figure 2) and thus, influences both activity and selectivity of the respective variant [46]. In analogy to this work, the variant F87V/A328L, which revealed the highest activity to 3-methylanisole (**1**), was chosen for the combination with an additional mutation at position L437. Additional mutations in position 437 were previously shown to be beneficial for the synthesis of perillyl alcohol from (4*R*)-limonene, presumably due to the strong influence of the respective amino

acid at this position on the orientation of the substrate in the active site [46]. The wild-type leucine was replaced by alanine, phenylalanine, isoleucine and valine, as substrate-interacting amino acids in P450s are preferentially hydrophobic [24]. The respective CYP102A1 triple variants were finally investigated concerning the conversion of the 3-methylanisole (1) (Table 1 and Table S2), as well as the compounds 3-methoxybenzyl alcohol (2), 4-methylguaiacol (3) and vanillyl alcohol (4). While 3-methoxybenzyl alcohol (2), 4-methylguaiacol (3) and vanillyl alcohol (4) were not converted by any of the triple variants (data not shown), the mutations of L437 clearly influenced the enzyme activity and selectivity in the conversion of 3-methylanisole (1). Replacement of leucine at amino acid position 437 by alanine or phenylalanine dramatically decreased the total conversion of 3-methylanisole (1), whereas isoleucine and valine at position 437 had no effect on the enzymatic activity. However, in this case, the product distribution was different. About twice the amount of product 3-methoxybenzyl alcohol (2) was formed; the concentration of produced compound 4-methylguaiacol (3), 4-methoxy-2-methylphenol (6) and *m*-cresol (9) was reduced approximately by half; and the overoxidation product methylhydroquinone (10), generated via 9, increased slightly. None of the investigated CYP102A1 variants was able to catalyse the second reaction step of the cascade, accepting either 3-methoxybenzyl alcohol (2) or 4-methylguaiacol (3) as a substrate.

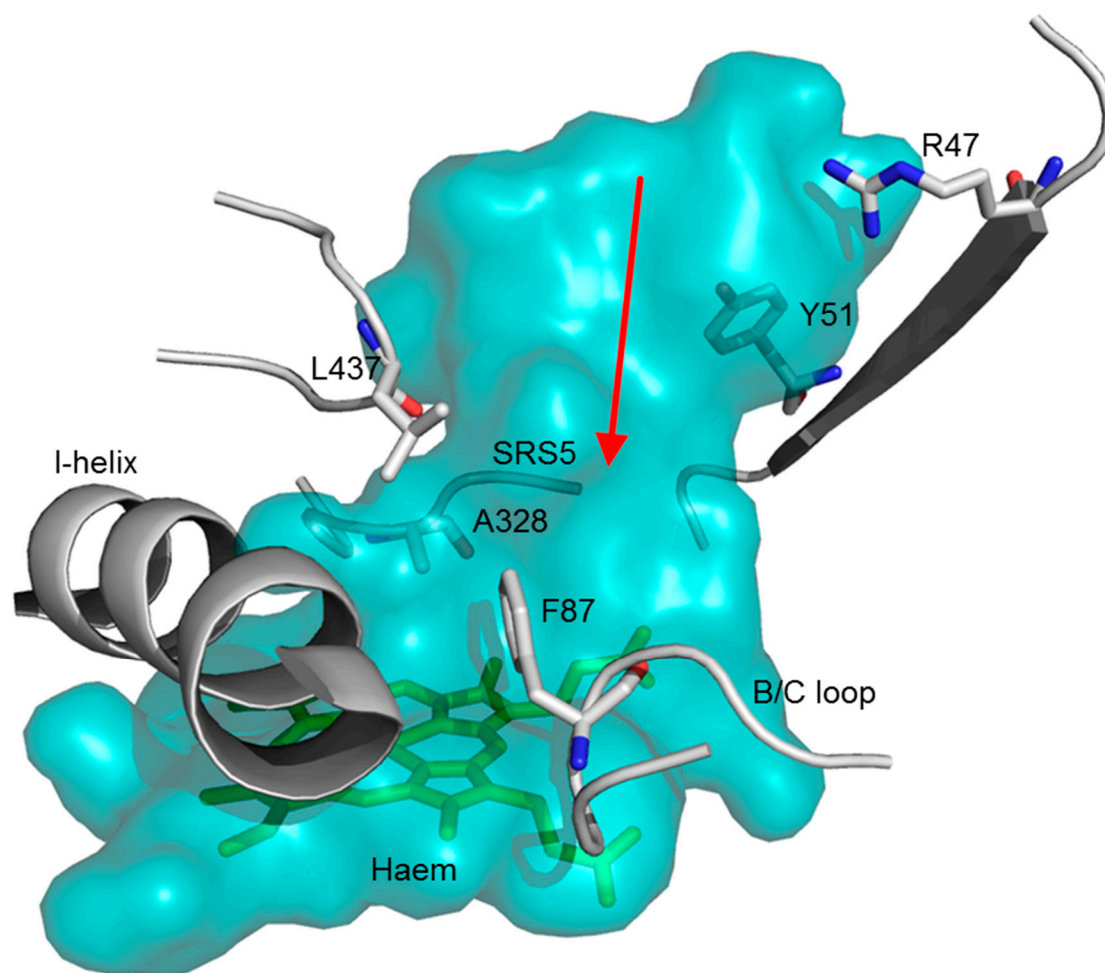


**Figure 2.** Haem access region in CYP102A1 (PDB ID: 1BU7, chain A). The image was generated by PyMOL. Active site residues, including the haem group (green), a section of the I-helix, B/C loop with F87, a section of the substrate recognition site 5 (SRS5) with A328, residue L437 (positioned at the substrate entrance to the active site cavity) and substrate channel residues R47 and Y51 are shown. The entrance route of the substrate to the active site is indicated by a red arrow.

So far many of the variants showed conversion of 3-methylanisole (**1**) to intermediate product 3-methoxybenzyl alcohol (**2**) and 4-methylguaiacol (**3**) in various amounts in our study. Unfortunately, due to the low selectivity of the enzyme variants, intense byproduct formation was also detected. The aromatic hydroxylation in *para* position to the methyl group is less favoured compared to the benzylic hydroxylation of substrate 3-methylanisole (**1**), as intermediate product 3-methoxybenzyl alcohol (**2**) was detected in higher amounts than intermediate product 4-methylguaiacol (**3**) (product formation of about 22% compared to less than 3%, respectively).

### 2.3. Molecular Dynamics Simulation

Based on the enzymatic preference for the benzylic hydroxylation compared to the aromatic hydroxylation in *para* position to the methyl group, as mentioned above, the second pathway via benzylic hydroxylation of the intermediate compound 4-methylguaiacol (**3**) to the product vanillyl alcohol (**4**) was chosen for further investigation. Though many of the applied single, double and triple variants of CYP102A1 showed methyl group hydroxylation of 3-methylanisole (**1**) and in spite of the fact that 3-methylanisole (**1**) differs from 4-methylguaiacol (**3**) by only one hydroxyl group, the latter is not converted by any of the minimal library variants. In order to unveil whether 4-methylguaiacol (**3**) is able to bind in productive orientations in the active site cavity of CYP102A1 variant F87V/A328I, multiple 100 ns molecular dynamics (MD) simulations (30) of the enzyme substrate complex were carried out. In the simulations, 4-methylguaiacol (**3**) was frequently observed in three different regions of the substrate binding cavity (Figure S1). In five out of 15 simulations, 4-methylguaiacol (**3**) stayed close to its initial position in a distance of 10 Å from the activated oxygen. In six simulations, 4-methylguaiacol (**3**) approached the activated oxygen in different orientations to a distance suitable for oxidation. As an example, in one simulation 4-methylguaiacol (**3**) moved towards the haem during the first 10 ns and stayed stable for the remaining 90 ns with its ring methyl group exposed to the activated haem oxygen with a C-OFe distance < 4 Å (Figure S2). This indicates that 4-methylguaiacol (**3**) binds in a productive conformation to the active site of variant F87V/A328I. Interestingly, in the remaining four simulations, 4-methylguaiacol (**3**) moved from its initial position to a pocket formed by the  $\beta_1$  sheet and the A' helix. The pocket is located in ~20 Å distance from the active site haem in the substrate access channel. There, 4-methylguaiacol (**3**) was stabilised by polar interaction/hydrogen bonds with residues R47 and Y51 (Figure S3). The stabilisation of the molecule in this pocket might hamper its approach to the haem active site, which could explain the lacking activity of the variant towards 4-methylguaiacol (**3**). As a consequence, the substitution of R47 and Y51 to nonpolar residues should abolish these polar interactions, and therefore facilitate the approach of 4-methylguaiacol (**3**) to the active site enabling its conversion.

### 2.4. Screening of Quadruple CYP102A1 Variants for Substrate Conversion

As a result of the MD simulations, R47L/Y51F-mutations were inserted in the previously investigated single and double variants and in one of the triple variants, which showed the highest activity for the conversion of 3-methylanisole (**1**). Subsequently, these quadruple variants and the one quintuple variant were screened for the conversion of 4-methylguaiacol (**3**) as well as 3-methylanisole (**1**), 3-methoxybenzyl alcohol (**2**) and vanillyl alcohol (**4**). 4-Methylguaiacol (**3**), which was neither accepted as a substrate by the CYP102A1 wild-type nor by any of the previously applied CYP102A1 single, double and triple variants, was converted by all of the designed R47L/Y51F-variants, except for R47L/Y51F and R47L/Y51F/A328L (Table S3). The highest conversion of 4-methylguaiacol (**3**) with concomitant production of vanillyl alcohol (**4**) was measured with the variant R47L/Y51F/F87V/A328V (4.5%). This indicates that the blocking of the substrate channel by hydrogen bond formation with 4-methylguaiacol (**3**) could be overcome. Besides, for all quadruple variants and the one quintuple variant, a very small peak of an unknown byproduct was detected (data not shown). Due to the missing reference substance, the amount of this compound could not be determined. Whilst compounds 3-methoxybenzyl alcohol (**2**) and vanillyl alcohol (**4**) were not converted at all, conversion of 3-methylanisole (**1**) was

achieved with all variants (Table 1 and Table S2). The R47L/Y51F-variant of the CYP102A1 wild-type showed only little conversion of 3-methylanisole (**1**). Compared to the respective single, double and triple variants, variants with the additional mutations R47L and Y51F demonstrated varying performance in enzyme activity. Only variant R47L/Y51F/F87V/A328V displayed no change in activity and product distribution compared to the respective double variant (F87V/A328V). The highest total conversion of 50% was detected for the quintuple variant R47L/Y51F/F87V/A328L/L437I. Furthermore, product distribution of the conversion of 3-methylanisole (**1**) with the R47L/Y51F-variants compared to the variants without these mutations did not change dramatically, except that the overoxidation product methylhydroquinone (**10**) was detected for some more variants.

### 2.5. In Vitro One-Pot Cascade Reactions

As CYP102A1 variants for both reaction steps from 3-methylanisole (**1**) to product vanillyl alcohol (**4**) have now been identified, a one-pot two-step biocatalytic cascade sequence of cytochrome P450 monooxygenase-catalysed oxidation reactions was set up with the aim of the production of vanillyl alcohol (**4**). For this purpose, the CYP102A1 variants A328L and R47L/Y51F/F87V/A328V were chosen, as they were shown to be the most efficient variants concerning the conversion of 2 mM of 3-methylanisole (**1**) to intermediate product 4-methylguaiacol (**3**) and further conversion of this compound to product vanillyl alcohol (**4**), respectively. 3-Methylanisole (**1**) was converted to about 25% with 4-methoxy-2-methylphenol (**6**) as main product (19.3%) and small amounts of intermediate 4-methylguaiacol (**3**) (1.2%) (Table 2). A successive addition of the second enzyme after half of the reaction time led to an increase in total conversion up to about 30%. Besides, the amount of produced compounds 4-methylguaiacol (**3**) and 4-methoxy-2-methylphenol (**6**) increased slightly, whereas the formation of compounds 3-methoxybenzyl alcohol (**2**) and *m*-cresol (**9**) (data not shown) decreased. However, the intended product vanillyl alcohol (**4**) could not be detected in any of the two reaction setups by GC–FID analysis. This was also confirmed by HPLC analysis of the samples (data not shown). For this reason, we investigated a different cascade reaction setup with a known vanillyl alcohol oxidase (VAO) from *P. simplicissimum* as a second enzyme in combination with the CYP102A1 variant A328L. This VAO is not only known to catalyse the conversion of vanillyl alcohol (**4**) to vanillin (**5**), but also to catalyse the conversion of 4-methylguaiacol (**3**) via vanillyl alcohol (**4**) to vanillin (**5**). As there is some information about improved variants [33], we chose the VAO variant F454Y according to the published data and created it by site-directed mutagenesis. A comparison of the VAO wild-type and F454Y variant in an in vitro conversion of 4-methylguaiacol (**3**) confirmed the much higher activity of the single variant F454Y (data not shown). Therefore, VAO\_F454Y was applied in combination with A328L (best CYP102A1 variant for conversion of 3-methylanisole (**1**) to intermediate 4-methylguaiacol (**3**) in the in vitro one-pot cascade reactions with VAO and P450 (Table 2). We assume that this results from the low amount of 4-methylguaiacol (**3**) that is produced by A328L in the first reaction step and the competitive conversion of 3-methylanisole (**1**) and 4-methylguaiacol (**3**), with a preference for 3-methylanisole (**1**), by the R47L/Y51F/F87V/A328V variant in the second reaction step. A successive addition of the second enzyme after half of the reaction time improved the total conversion but was not sufficient for the synthesis of vanillyl alcohol (**4**).

Though the total conversion and the formation of 4-methoxy-2-methylphenol (**6**) did not change dramatically compared to the setup with the two CYP102A1 variants, in the system with the VAO variant F454Y as a second enzyme, less 4-methylguaiacol (**3**) was detected. Moreover, the final target product vanillin (**5**) could be detected by GC–FID. The formation of vanillyl alcohol (**4**) was not observed. This clearly indicates that A328L catalysed the conversion of 3-methylanisole (**1**) to 4-methylguaiacol (**3**), which was then oxidised by the VAO variant F454Y via the intermediate product vanillyl alcohol (**4**) to the product vanillin (**5**) (complete conversion of vanillyl alcohol to vanillin). Byproducts *m*-cresol (**9**) and methylhydroquinone (**10**) were only detected in very low amounts (data not shown).

**Table 2.** Results of the in vitro one-pot conversion of 3-methylanisole (1) with a combination of the CYP102A1 variants A328L and R47L/Y51F/F87V/A328V and a combination of A328L and the vanillyl alcohol oxidase (VAO) variant F454Y.

Enzymes	Reaction Time (h)	Product Yield (% of Initial Substrate)				Total Conversion (%)
		2	3	5	6	
A328L	2	2.2 ± 0.1	1.2 ± 0.1	–	19.3 ± 1.3	24.7 ± 1.6
R47L/Y51F/F87V/A328V	1 + 1	1.2 ± 0.2	2.4 ± 0.5	–	25.6 ± 4.8	30.3 ± 5.7
A328L	2	<1	<1	<1	19.8 ± 2.7	22.9 ± 3.1
VAO_F454Y	1 + 1	1.0 ± 0.1	<1	1.2 ± 0.1	25.0 ± 2.2	29.0 ± 2.5

–, not detected or <0.05%; 2, 3-methoxybenzyl alcohol; 3, 4-methylguaiacol; 5, vanillin; 6, 4-methoxy-2-methylphenol; and conversion time “1+1” indicates addition of the second enzyme after 1 h. Negative controls showed no conversion. Reactions were performed in triplicates using a volume of 1 mL in Tris-HCl buffer pH 7.5 (50 mM). Substrate was added at a final concentration of 2 mM from a 100-mM stock solution in dimethyl sulphoxide (DMSO). CYP102A1 and variants thereof were used as lysate at a final concentration of 1 µM. Reactions were run at 30 °C and 180 rpm for 2 h. Samples were derivatised and analysed by GC-FID.

## 2.6. In Vivo Cascade Reactions

Finally, we were interested in the conversion of 3-methylanisole (1) to vanillin (5) in vivo with *E. coli* as expression host. The advantages of an in vivo conversion with whole cells compared to an in vitro system are especially the higher stability of the enzymes in a cellular system and the employment of the NADPH cofactor and cofactor regeneration system of the host cells. Therefore, *E. coli* BL21(DE3) cells were transformed with plasmids harboring genes for the enzymes CYP102A1\_A328L and VAO\_F454Y. After protein expression, the cells were harvested and applied in the whole-cell conversion setup. The results of the in vivo biotransformation are shown in Figure 3 and Table S4. 4-Methoxy-2-methylphenol (6), the main byproduct in all of our earlier investigations, was the only product detected during the first hour of reaction time and stayed the main product throughout the whole reaction. Besides, the intermediate products 3-methoxybenzyl alcohol (2) and 4-methylguaiacol (3), byproduct *m*-cresol (9) and the target product vanillin (5) were detected after 3 h. Very interestingly, the product yield of vanillin (5) increased in the course of reaction time, whilst the concentration of 3-methoxybenzyl alcohol (2), 4-methylguaiacol (3) and *m*-cresol (9) stayed at a very low level and vanillyl alcohol (4) was not detected at all. These findings confirm the functionality of the reaction pathway from 3-methylanisole (1) to vanillin (5) in vivo. However, after 12 h, the total conversion (11.7%) and the yield of product 5 (1.1%) reached the maximum, though glycerol and glucose were supplemented again to the biotransformation medium. The successful formation of vanillin (5) was confirmed by GC-MS analysis and comparison of the fragmentation pattern of the respective product peak and a vanillin reference (Figure S4).

The high demand for natural flavor has resulted in the development of novel alternative production processes for natural vanillin. Natural vanillin is extracted from the orchids *Vanilla planifolia*, *Vanilla tahitiensis*, and *Vanilla pompon* [3,47]. However, the production of natural vanillin from vanilla pods is very time consuming and expensive. Moreover, weather conditions as well as plant diseases directly influence the market volume and process for vanillin extracted from vanilla pods. Recently, the conversion of certain raw material to synthesise vanillin through biotechnological means has been presented. Vanillin produced from alternate natural raw materials can be classified as natural product. Biotechnological approaches for vanillin production are mostly based on conversion of lignin, phenolic stilbenes, isoeugenol, eugenol, ferulic acid or aromatic amino acids. In view of the above, it is considered desirable to further explore the raw materials that would lead to a possible novel vanillin production pathway. In this work, the microbial transformation of the cheap and readily available substrate 3-methylanisole to synthesise vanillin has been studied. This substrate has shown promise due to its production by both chemical and biotechnological processes. In the biotechnology-based approach, *m*-cresol, biosynthesised from acetyl-CoA and malonyl-CoA, can be

converted to the desired 3-methylanisole with an *O*-methyltransferase, which is then deployed as alternative natural raw material for the microbial production of vanillin.

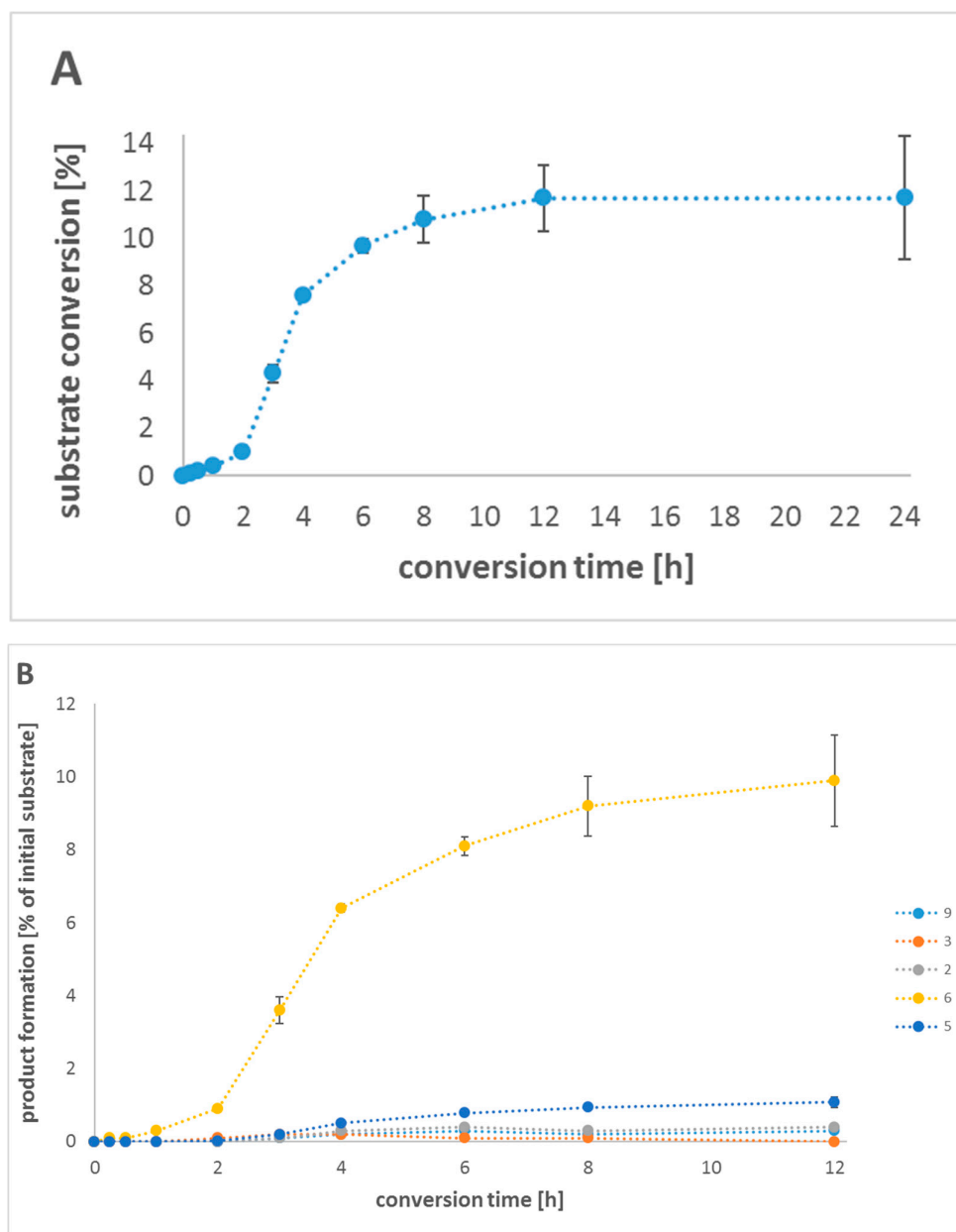


**Figure 3.** Total conversion within 24 h reaction time (A) and product formation within 12 h reaction time (B) of the in vivo 3-methylanisole (1) cascade conversion with a combination of the enzymes CYP102A1\_A328L and VAO\_F454Y. Due to the fact that no further conversion of substrate after 12 h reaction time was observed, product formation within this time frame is shown. 2, 3-methoxybenzyl alcohol; 3, 4-methylguaiacol; 5, vanillin; 6, 4-methoxy-2-methylphenol; 9, *m*-cresol.

### 3. Materials and Methods

#### 3.1. Materials

All chemicals were purchased in analytical-reagent grade or higher quality. Tryptone from casein was obtained from Fluka (Buchs, Switzerland), yeast extract and vanillin from Roth (Karlsruhe, Germany) and  $\beta$ -NADPH tetrasodium salt from Acros Organics (Geel, Belgium). Glucose-6-phosphate dehydrogenase from *Saccharomyces cerevisiae* was purchased from Roche Diagnostics (Mannheim, Germany).

3-Methylanisole, 4-methylguaiacol, 3-methoxybenzyl alcohol, vanillyl alcohol, vanillin and 3-methoxy-5-methylphenol were obtained from Alfa Aesar (Karlsruhe, Germany), 2-methoxy-6-methylphenol from Frinton Laboratories (Hainesport, NJ, USA), D-Glucose-6-phosphate disodium salt hydrate, *m*-cresol, 4-methoxy-2-methylphenol, methylhydroquinone and all other chemicals, solvents and buffer components from Sigma-Aldrich (Schnelldorf, Germany). Oligonucleotides were bought from Metabion (Martinsried, Germany) in salt-free form.

### 3.2. Plasmids and Strains

*Escherichia coli* DH5 $\alpha$  from Invitrogen (now Life Technologies, Darmstadt, Germany) was used as host for cloning. For recombinant gene expression, the plasmids pET-22b(+), pET-28a(+) and the strain *E. coli* BL21(DE3) from Novagen (Madison, Wisconsin, USA) were used as expression vectors and expression host, respectively.

### 3.3. Molecular Biology Techniques and Enzyme Expression

General molecular biological and microbiological experiments were carried according to standard procedures [48]. The QuikChange<sup>TM</sup> site-directed mutagenesis kit from Stratagene (La Jolla, California, USA) was used to introduce site-directed mutations, following the manufacturer's protocol. Heterologous expression of the CYP102A1 wild-type and variants in *E. coli* was done as reported previously [49]. Expression and cultivation was performed as described in the PhD thesis of Tobias Klaus (University of Stuttgart, Germany) [50]. The codon-optimised *vaoA* gene from *P. simplicissimum* was obtained as a synthetic gene (Life Technologies GmbH, Darmstadt, Germany). After cloning the wild-type *vaoA* gene into the *Nde*I and *Xho*I cloning sites of the T7 promoter-based pET-22b(+) vector, the variant F454Y was constructed by site-directed mutagenesis following the manufacturer's protocol, mentioned above. Successful cloning was verified by automated DNA-sequencing (GATC Biotech, Konstanz, Germany). For protein expression, the pET-22b(+)\_VAO\_F454Y vector construct was transformed into competent *E. coli* BL21(DE3) cells and transformants were selected on LB agar plates with ampicillin (100  $\mu$ g/mL). A volume of 400 mL LB medium supplemented with 100  $\mu$ g/mL of ampicillin was inoculated with 2 mL overnight culture—grown from a single colony—and grown at 37 °C and 180 rpm. At an OD<sub>600</sub> of 0.7–0.8, the culture was supplemented with 0.5 mM isopropyl- $\beta$ -D-thiogalactopyranoside (IPTG) and grown for another 18 h at 20 °C and 140 rpm. Harvest of cells was done by centrifugation (10,800  $\times$  *g*, 20 min, 4 °C), followed by resuspension in buffer solution (50 mM Tris-HCl buffer pH 7.5 containing 500 mM NaCl, 5% glycerol, 0.1 mM phenylmethylsulphonyl fluoride (PMSF)). Disruption of cells was done by sonication on ice (6  $\times$  1 min, interspaced by 30 s). Subsequently, the cell debris was removed by centrifugation (37,000  $\times$  *g*, 30 min, 4 °C), and the soluble protein fraction was recovered and filtered through a 0.45- $\mu$ m sterile filter.

### 3.4. Determination of Protein Concentration

The concentrations of the CYP102A1 variants were determined by the CO differential spectral assay as described previously [51,52] using an extinction coefficient of 91 mM<sup>-1</sup> cm<sup>-1</sup>. The Bradford protein assay was used for the determination of total protein concentration [53].

### 3.5. In Vitro Biotransformations

Biotransformations were performed as described in the PhD thesis of Tobias Klaus (University of Stuttgart, Germany) [50] using a final volume of 1 mL in 50 mM Tris-HCl buffer pH 7.5, containing 1 mM MgCl<sub>2</sub>, 5 mM glucose-6-phosphate (G6P) and 5 U/mL glucose-6-phosphate dehydrogenase (G6PDH) for cofactor regeneration. For biotransformations, substrates 3-methylanisole, 4-methylguaiacol, 3-methoxy-benzyl alcohol and vanillyl alcohol were added at a final concentration of 0.5 mM (from a 25 mM stock solution in dimethyl sulphoxide). A concentration of 1  $\mu$ M or 0.5  $\mu$ M of CYP102A1 enzyme (lysate) was added for the conversion of 3-methylanisole or 4-methylguaiacol,

3-methoxybenzyl alcohol and vanillyl alcohol, respectively. The reaction was started by the addition of 0.2 mM NADPH. Samples were incubated at 30 °C and 180 rpm for 2 h.

One-pot cascade reactions using CYP102A1 variants A328L and R47L/Y51F/F87V/A328V were conducted as described in the PhD thesis of Tobias Klaus (University of Stuttgart, Germany) [50] with CYP102A1 enzyme variants (lysate) and the substrate 3-methylanisole added at a final concentration of 1 µM and 2 mM, respectively. For further evaluation, in some experiments, the second enzyme variant was added after 1 h (total reaction time was 2 h). One-pot cascade reactions with a combination of the CYP102A1 variant A328L and the VAO variant F454Y were performed with VAO\_F454Y-lysate added at a final VAO-lysate protein concentration of 1 mg/mL. Lysate of empty vector expression (pET-22b(+)) or pET-28a(+) in *E. coli* BL21(DE3)) was used as a negative control for the in vitro biotransformations. Experiments were performed in triplicate.

### 3.6. In Vivo Biotransformations

Whole-cell biotransformations were performed as described in the PhD thesis of Tobias Klaus (University of Stuttgart, Germany) [50]. Competent *E. coli* BL21(DE3) cells were transformed with the plasmids pET-28a(+)\_CYP102A1\_A328L and pET-22b(+)\_VAO\_F454Y. Protein expression was performed as described above with minor modifications. LB medium was supplemented with both kanamycin (30 µg/mL) and ampicillin (100 µg/mL) and protein expression was induced by adding 1 mM IPTG, 0.1 mM 5-aminolevulinic acid and 0.1 mM FeSO<sub>4</sub>. After incubation at 20 °C and 140 rpm for 18 h, cells were harvested by centrifugation (2700 × *g*, 20 min, 4 °C), washed twice with 50 mM Tris-HCl buffer pH 7.5, followed by resuspension in biotransformation medium. In vivo biotransformations were carried out in 100 mL shake flasks with a volume of 30 mL biotransformation medium. For bioconversions, fresh cell suspension (50 g<sub>cww</sub>/L) in 50 mM Tris-HCl buffer pH 7.5 with 1% (*w/v*) glycerol, 0.4% (*w/v*) D-glucose, 30 µg/mL kanamycin and 100 µg/mL ampicillin was prepared. Biotransformations were started by the addition of substrate 3-methylanisole (from a 200 mM stock solution in dimethyl sulfoxide) at a final concentration of 4 mM and incubated at 30 °C and 180 rpm for 24 h. After 12 h reaction time, cells were fed with a glycerol/glucose mixture (1% (*w/v*) glycerol, 0.4% (*w/v*) D-glucose). For analysis, samples were collected at time points 0, 15 and 30 min and 1, 2, 3, 4, 6, 8, 12 and 24 h after substrate addition. As negative controls, *E. coli* BL21(DE3) cells transformed with empty vectors pET-28a(+) and pET-22b(+) were used. Experiments were performed in triplicate.

### 3.7. Sample Treatment

Preparation of samples for GC or HPLC analysis was conducted as described in the PhD thesis of Tobias Klaus (University of Stuttgart, Germany) [50]. Substrate conversion was stopped with 20 µL concentrated HCl. For initial library screening by high-performance liquid chromatography (HPLC), substrate and products were extracted from the aqueous reaction mixture by the addition of 0.5 g of K<sub>2</sub>CO<sub>3</sub> and 0.5 mL of a 40/60 (% *v/v*) mixture of *n*-hexane/2-propanol. Samples were mixed for 2 min and centrifuged for 3 min at 20,200 × *g*. For analysis, 100 µL of organic phase was mixed with 100 µL of *n*-hexane. In order to determine substrate conversion and product distribution, transformations were extracted using 0.25 mL ethyl acetate containing the internal standard benzaldehyde (0.1 mM) or catechol (0.5 mM) for gas chromatography (GC) analysis or HPLC analysis, respectively.

### 3.8. GC Analysis

GC analyses were performed as described in the PhD thesis of Tobias Klaus (University of Stuttgart, Germany) [50]. Biotransformations were analysed on a GC-FID (GC-2010 from Shimadzu (Kyoto, Japan) with flame ionization detector) equipped with a DB-5 capillary column (length, 30 m; internal diameter, 0.25 mm; film thickness, 0.25 µm) from Agilent Technologies (Waldbronn, Germany). Hydrogen was used as carrier gas (flow rate, 0.88 mL/min; linear velocity, 30 cm/s). The injector and detector temperatures were set at 200 °C and 330 °C, respectively. The temperature program of

the column oven was as follows: 100 °C for 3 min, 10 °C/min to 190 °C, 75 °C/min to 320 °C and hold for 3 min. Reference materials were used for the determination of substrate conversion and product distribution. In this case, solutions with 0.01–0.5 mM reference substances in 50 mM Tris-HCl buffer pH 7.5 were extracted with ethyl acetate containing internal standard, followed by analysis with GC–FID to obtain straight-line calibration plots (determination of the internal response factor).

In addition to GC–FID, GC–MS measurements were performed on a GC-2010 with GCMS-QP2010 from Shimadzu (Kyoto, Japan) equipped with a DB-5MS capillary column (length, 30 m; internal diameter, 0.25 mm; film thickness, 0.25 µm) from Agilent Technologies (Waldbronn, Germany). Helium was used as carrier gas (flow rate, 4.3 mL/min; linear velocity, 30 cm/s). The injector temperature was set at 250 °C. Mass spectra were collected using electrospray ionisation (70 eV). The temperature program of the column oven was as follows: 80 °C for 1 min, 60 °C/min to 140 °C, hold for 3 min, 20 °C/min to 160 °C, hold for 5 min, 75 °C/min to 320 °C and hold for 2 min. The use of reference materials and analysis of respective fragmentation patterns supported the identification of reaction products.

### 3.9. HPLC Analysis

HPLC analyses were performed as described in the PhD thesis of Tobias Klaus (University of Stuttgart, Germany) [50]. Biotransformations were analysed by normal phase high-performance liquid chromatography on a 1200 Series HPLC from Agilent Technologies (Waldbronn, Germany) equipped with a Luna Silica 5-µm column (particle size, 5 µm; pore size, 100 Å; length, 150 mm; inner diameter, 4.6 mm) from Phenomenex (Aschaffenburg, Germany). A mixture of 2-propanol with 0.2 M formic acid (A), 2-propanol (B) and *n*-hexane (C) was used as mobile phase. Gradient elution was applied with solution A (constant 5%), solution B (0%–25% in 4 min, 25%–45% in 4 min) and solution C to complement to 100% at 30 °C and a flow rate of 0.8 mL/min. For initial library screening, 40 µL of extracted sample was injected and analysed at a wavelength of 272 nm. The analysis of 4-methylguaiaicol conversion and product distribution was performed at 280 nm with 15 µL of extracted sample. For calibration, standard solutions in the range of 0.01–0.5 mM reference substances in 50 mM Tris-HCl buffer pH 7.5 were prepared and were extracted with ethyl acetate containing internal standard.

### 3.10. Molecular Dynamics Simulations

Molecular dynamics (MD) simulations were performed with the GROMACS 4.5.3 software (Department of Biophysical Chemistry, University of Groningen, Groningen, Netherlands) [54,55] at  $T = 298\text{K}$  and 1 bar, using the leap-frog integrator [56] with a time step of 2 fs. Systems were equilibrated for 2 ns with position restraints on the protein and the substrate during the first 50 ps, while applying Nose-Hoover [57,58] temperature coupling and Parrinello-Rahman [59] pressure coupling. This coupling scheme was also applied to the 100-ns production runs that were the basis for analysis. Independent coupling for the protein group, the substrate group and the water/ions group were applied every 5 ps for pressure and every 0.5 ps for temperature. Hydrogen-bond lengths were constrained with the LINCS algorithm [60]. Long-range electrostatics was calculated with the particle-mesh Ewald method (PME) [61,62]. Lennard-Jones interactions were treated with a cutoff and capped at 1.2 nm. The CYP102A1 crystal structure PDB ID: 1BU7A (1.65 Å resolution) was chosen as the protein coordinate file. The Pymol 0.99 program [63] was used to introduce the amino acid exchanges at positions 87 and 328. The protein was parameterised with the Amber03 force field [64], with the exception of the haem group, which was parameterised as previously described [24]. The substrate was manually placed into the active site in a distance of 10 Å from the haem center. Substrate parameters were derived from the AMBER03 force field and the general AMBER force field (GAFF) [65] as needed, while charge parameters were calculated using the RESP ESP charge Derive Server (REDS) [66], using the GAMESS-US quantum mechanics program [67] in conjunction with the RESP-A1B charge model.

Water was described by the SPC/E model [68]. Counter-ions were added to neutralise the overall system charge.

#### 4. Conclusions

This research generated a variety of CYP102A1 single, double and triple variants to oxidise the starting material 3-methylanisole to vanillyl alcohol, an important precursor of vanillin. Variants were identified catalysing the conversion of 3-methylanisole (1) to both 3-methoxybenzyl alcohol (2) and 4-methylguaiacol (3). MD simulations have identified two additional mutation sites, and variants thereof were successfully applied for the conversion of 4-methylguaiacol (3) to vanillyl alcohol (4). Successful synthesis of vanillin (5) was finally achieved both in an in vitro and an in vivo whole-cell cascade reaction, starting with 3-methylanisole (1) as a substrate and employing a combination of variants of two different enzymes (CYP102A1\_A328L and VAO\_F454Y). The in vivo synthesis of vanillin (5) reached a maximum of 1.1% after 12 h. Thus, as a proof of principle, a new biotechnological pathway for the synthesis of vanillin (5) is reported in this work. Further optimisations of this cascade synthesis need to be addressed in the future.

**Supplementary Materials:** The following are available online at <http://www.mdpi.com/2073-4344/9/3/252/s1>, Figure S1: Regions in CYP102A1 variant F87V/A328I active site cavity where 4-methylguaiacol (3) was frequently observed during molecular dynamics (MD) simulations. The orange molecule shows the starting position, green—the region close to the haem center and blue—the pocket formed by the  $\beta$ 1 sheet and the A' helix. The substrate access channel is indicated by a red arrow. (B) is zoomed in on (A). Figure S2: Distance of 4-methylguaiacol (3) carbon atoms from the activated oxygen of the haem in a 100 ns MD run. The molecule approaches the haem oxygen to a distance  $<4 \text{ \AA}$  (C7) where it stays stable for 90 ns. Lines show a moving average of 20 data points. Figure S3: Representation of four exemplary MD simulations from a pool of 15 MD simulations. The distance between all possible hydrogen bond donors and acceptors of 4-methylguaiacol (3) and the side chain of Y51 (green, red and magenta lines) and R47 (all remaining lines) are shown. A hydrogen bond is considered present at a hydrogen bond donor to acceptor distance  $\leq 3.5 \text{ \AA}$ . Lines show a moving average of 20 data points. Figure S4: GC–MS analysis chromatogram (A) and fragmentation patterns of reference compound (B) (0.05 mM vanillin) and sample (C) (after 12 h conversion time) of the in vivo biotransformations. Table S1: Initial screening results for the conversion of 3-methylanisole (1) catalysed by all 24 variants plus wild type of the CYP102A1 minimal mutant library. Lysate of empty vector expression (pET-22b(+), pET-28a(+)) was used as a negative control and showed no conversion. Table S2: Results of the conversion of 3-methylanisole (1) with all investigated variants of CYP102A1. Table S3: Results of the conversion of 4-methylguaiacol (3) with R47L/Y51F-variants of CYP102A1. Table S4: Results of the in vivo conversion of 3-methylanisole (1) with a combination of the CYP102A1 variant A328L and the vanillyl alcohol oxidase (VAO) variant F454Y.

**Author Contributions:** T.K. performed the experiment, T.H. screened the first enzyme library, A.S. performed molecular dynamics simulations and T.K., B.M.N. and B.H. wrote the paper.

**Funding:** This work was supported by the German Federal Ministry of Education and Research (BMBF) in the frame of the “Systems Biology in Pseudomonas for Industrial Biocatalysis” project. We want to thank Jürgen Pleiss for bioinformatic support of this study.

**Conflicts of Interest:** The authors declare no conflict of interest.

#### References

1. Priefert, H.; Rabenhorst, J.; Steinbuchel, A. Biotechnological production of vanillin. *Appl. Microbiol. Biotechnol.* **2001**, *56*, 296–314. [[CrossRef](#)] [[PubMed](#)]
2. Walton, N.J.; Mayer, M.J.; Narbad, A. Vanillin. *Phytochemistry* **2003**, *63*, 505–515. [[CrossRef](#)]
3. Kaur, B.; Chakraborty, D. Biotechnological and molecular approaches for vanillin production: A review. *Appl. Biochem. Biotechnol.* **2013**, *169*, 1353–1372. [[CrossRef](#)]
4. Banerjee, G.; Chattopadhyay, P. Vanillin biotechnology: The perspectives and future. *J. Sci. Food Agric.* **2019**, *99*, 499–506. [[CrossRef](#)]
5. Gallage, N.J.; Møller, B.L. Vanillin-bioconversion and bioengineering of the most popular plant flavor and its de novo biosynthesis in the vanilla orchid. *Mol. Plant* **2015**, *8*, 40–57. [[CrossRef](#)]
6. Furuya, T.; Miura, M.; Kino, K. A coenzyme-independent decarboxylase/oxygenase cascade for the efficient synthesis of vanillin. *ChemBioChem* **2014**, *15*, 2248–2254. [[CrossRef](#)]

7. Furuya, T.; Kuroiwa, M.; Kino, K. Biotechnological production of vanillin using immobilized enzymes. *J. Biotechnol.* **2017**, *243*, 25–28. [[CrossRef](#)] [[PubMed](#)]
8. Girvan, H.M.; Munro, A.W. Applications of microbial cytochrome P450 enzymes in biotechnology and synthetic biology. *Curr. Opin. Chem. Biol.* **2016**, *31*, 136–145. [[CrossRef](#)] [[PubMed](#)]
9. Cryle, M.J.; Stok, J.E.; De Voss, J.J. Reactions catalyzed by bacterial cytochromes P450. *Aust. J. Chem.* **2003**, *56*, 749–762. [[CrossRef](#)]
10. Hammer, S.C.; Knight, A.M.; Arnold, F.H. Design and evolution of enzymes for non-natural chemistry. *Curr. Opin. Green Sustain. Chem.* **2017**, *7*, 23–30. [[CrossRef](#)]
11. Arnold, F.H. Directed Evolution: Bringing New Chemistry to Life. *Angew. Chem. Int. Ed.* **2018**, *57*, 4143–4148. [[CrossRef](#)]
12. Brandenburg, O.F.; Fasan, R.; Arnold, F.H. Exploiting and engineering hemoproteins for abiological carbene and nitrene transfer reactions. *Curr. Opin. Biotechnol.* **2017**, *47*, 102–111. [[CrossRef](#)]
13. Narhi, L.O.; Fulco, A.J. Identification and characterization of two functional domains in cytochrome P450-BM3, a catalytically self-sufficient monooxygenase induced by barbiturates in *Bacillus megaterium*. *J. Biol. Chem.* **1987**, *262*, 6683–6690.
14. Miura, Y.; Fulco, A.J. (Omega-2) hydroxylation of fatty acids by a soluble system from *Bacillus megaterium*. *J. Biol. Chem.* **1974**, *249*, 1880–1888.
15. Urlacher, V.B.; Lutz-Wahl, S.; Schmid, R.D. Microbial P450 enzymes in biotechnology. *Appl. Microbiol. Biotechnol.* **2004**, *64*, 317–325. [[CrossRef](#)]
16. Fasan, R. Tuning P450 Enzymes as Oxidation Catalysts. *ACS Catal.* **2012**, *2*, 647–666. [[CrossRef](#)]
17. O’Hanlon, J.A.; Ren, X.; Morris, M.; Wong, L.L.; Robertson, J. Hydroxylation of anilides by engineered cytochrome P450-BM3. *Org. Biomol. Chem.* **2017**, *15*, 8780–8787. [[CrossRef](#)]
18. Denard, C.A.; Ren, H.; Zhao, H. Improving and repurposing biocatalysts via directed evolution. *Curr. Opin. Chem. Biol.* **2015**, *25*, 55–64. [[CrossRef](#)]
19. Zhou, H.; Wang, B.; Wang, F.; Yu, X.; Ma, L.; Li, A.; Reetz, M.T. Chemo- and Regioselective Dihydroxylation of Benzene to Hydroquinone Enabled by Engineered Cytochrome P450 Monooxygenase. *Angew. Chem. Int. Ed.* **2019**, *58*, 764–768. [[CrossRef](#)]
20. Dennig, A.; Weingartner, A.M.; Kardashliev, T.; Müller, C.A.; Tassano, E.; Schürmann, M.; Ruff, A.J.; Schwaneberg, U. An Enzymatic Route to  $\alpha$ -Tocopherol Synthons: Aromatic Hydroxylation of Pseudocumene and Mesitylene with P450 BM3. *Chem. A Eur. J.* **2017**, *23*, 17981–17991. [[CrossRef](#)]
21. Dennig, A.; Lülldorf, N.; Liu, H.; Schwaneberg, U. Regioselective o-hydroxylation of monosubstituted benzenes by P450 BM3. *Angew. Chem. Int. Ed.* **2013**, *52*, 8459–8462. [[CrossRef](#)]
22. Munday, S.D.; Dezvarei, S.; Lau, I.C.-K.; Bell, S.G. Examination of Selectivity in the Oxidation of ortho- and meta-Disubstituted Benzenes by CYP102A1 (P450 BM3) Variants. *ChemCatChem* **2017**, *9*, 2512–2522. [[CrossRef](#)]
23. Seifert, A.; Pleiss, J. Identification of selectivity-determining residues in cytochrome P450 monooxygenases: A systematic analysis of the substrate recognition site 5. *Proteins* **2009**, *74*, 1028–1035. [[CrossRef](#)]
24. Seifert, A.; Vomund, S.; Grohmann, K.; Kriening, S.; Urlacher, V.B.; Laschat, S.; Pleiss, J. Rational design of a minimal and highly enriched CYP102A1 mutant library with improved regio-, stereo- and chemoselectivity. *ChemBioChem* **2009**, *10*, 853–861. [[CrossRef](#)]
25. Whitehouse, C.J.C.; Bell, S.G.; Wong, L.-L. P450<sub>BM3</sub> (CYP102A1): Connecting the dots. *Chem. Soc. Rev.* **2012**, *41*, 1218–1260. [[CrossRef](#)]
26. Weber, E.; Seifert, A.; Antonovici, M.; Geinitz, C.; Pleiss, J.; Urlacher, V.B. Screening of a minimal enriched P450 BM3 mutant library for hydroxylation of cyclic and acyclic alkanes. *Chem. Commun.* **2011**, *47*, 944–946. [[CrossRef](#)]
27. Whitehouse, C.J.; Rees, N.H.; Bell, S.G.; Wong, L.L. Dearomatisation of o-xylene by P450-BM3 (CYP102A1). *Chemistry* **2011**, *17*, 6862–6868. [[CrossRef](#)]
28. Winter, R.T.; Van Beek, H.L.; Fraaije, M.W. The nose knows: Biotechnological production of vanillin. *J. Chem. Educ.* **2012**, *89*, 258–261. [[CrossRef](#)]
29. de Jong, E.; van Berkel, W.J.; van der Zwan, R.P.; de Bont, J.A. Purification and characterization of vanillyl-alcohol oxidase from *Penicillium simplicissimum*. A novel aromatic alcohol oxidase containing covalently bound FAD. *Eur. J. Biochem.* **1992**, *208*, 651–657. [[CrossRef](#)]

30. Fraaije, M.W.; Veeger, C.; van Berkel, W.J. Substrate specificity of flavin-dependent vanillyl-alcohol oxidase from *Penicillium simplicissimum*. Evidence for the production of 4-hydroxycinnamyl alcohols from 4-allylphenols. *Eur. J. Biochem.* **1995**, *234*, 271–277. [[CrossRef](#)]
31. Fraaije, M.W.; van den Heuvel, R.H.; Roelofs, J.C.; van Berkel, W.J. Kinetic mechanism of vanillyl-alcohol oxidase with short-chain 4-alkylphenols. *Eur. J. Biochem.* **1998**, *253*, 712–719. [[CrossRef](#)]
32. van den Heuvel, R.H.; Fraaije, M.W.; Laane, C.; van Berkel, W.J. Enzymatic synthesis of vanillin. *J. Agric. Food Chem.* **2001**, *49*, 2954–2958. [[CrossRef](#)]
33. van den Heuvel, R.H.; van den Berg, W.A.; Rovida, S.; van Berkel, W.J. Laboratory-evolved vanillyl-alcohol oxidase produces natural vanillin. *J. Biol. Chem.* **2004**, *279*, 33492–33500. [[CrossRef](#)]
34. Schrittwieser, J.H.; Sattler, J.; Resch, V.; Mutti, F.G.; Kroutil, W. Recent biocatalytic oxidation-reduction cascades. *Curr. Opin. Chem. Biol.* **2011**, *15*, 249–256. [[CrossRef](#)]
35. García-Junceda, E.; Lavandera, I.; Rother, D.; Schrittwieser, J.H. (Chemo)enzymatic cascades—Nature’s synthetic strategy transferred to the laboratory. *J. Mol. Catal. B Enzym.* **2015**, *114*, 1–6. [[CrossRef](#)]
36. Muschiol, J.; Peters, C.; Oberleitner, N.; Mihovilovic, M.D.; Bornscheuer, U.T.; Rudroff, F. Cascade catalysis—Strategies and challenges en route to preparative synthetic biology. *Chem. Commun.* **2015**, *51*, 5798–5811. [[CrossRef](#)]
37. Schrittwieser, J.H.; Velikogne, S.; Hall, M.; Kroutil, W. Artificial Biocatalytic Linear Cascades for Preparation of Organic Molecules. *Chem. Rev.* **2018**, *118*, 270–348. [[CrossRef](#)]
38. Gruber, P.; Marques, M.P.C.; O’Sullivan, B.; Baganz, F.; Wohlgenuth, R.; Szita, N. Conscious coupling: The challenges and opportunities of cascading enzymatic microreactors. *Biotechnol. J.* **2017**, *12*, 1–13. [[CrossRef](#)]
39. Otte, K.B.; Hauer, B. Enzyme engineering in the context of novel pathways and products. *Curr. Opin. Biotechnol.* **2015**, *35*, 16–22. [[CrossRef](#)]
40. Hepworth, L.J.; France, S.P.; Hussain, S.; Both, P.; Turner, N.J.; Flitsch, S.L. Enzyme Cascades in Whole Cells for the Synthesis of Chiral Cyclic Amines. *ACS Catal.* **2017**, *7*, 2920–2925. [[CrossRef](#)]
41. Carnell, A.J. Synthetic cascades by combining evolved biocatalysts and artificial enzymes. *ChemCatChem* **2014**, *6*, 958–960. [[CrossRef](#)]
42. Oberleitner, N.; Peters, C.; Muschiol, J.; Kadow, M.; Saß, S.; Bayer, T.; Schaaf, P.; Iqbal, N.; Rudroff, F.; Mihovilovic, M.D.; et al. An enzymatic toolbox for cascade reactions: A showcase for an in vivo redox sequence in asymmetric synthesis. *ChemCatChem* **2013**, *5*, 3524–3528. [[CrossRef](#)]
43. Wu, S.; Li, Z. Whole-Cell Cascade Biotransformations for One-Pot Multistep Organic Synthesis. *ChemCatChem* **2018**, 2164–2178. [[CrossRef](#)]
44. Sulistyaningdyah, W.T.; Ogawa, J.; Li, Q.S.; Maeda, C.; Yano, Y.; Schmid, R.D.; Shimizu, S. Hydroxylation activity of P450 BM3 mutant F87V towards aromatic compounds and its application to the synthesis of hydroquinone derivatives from phenolic compounds. *Appl. Microbiol. Biotechnol.* **2005**, *67*, 556–562. [[CrossRef](#)] [[PubMed](#)]
45. Shoji, O.; Kunimatsu, T.; Kawakami, N.; Watanabe, Y. Highly selective hydroxylation of benzene to phenol by wild-type cytochrome P450-BM3 assisted by decoy molecules. *Angew. Chem. Int. Ed.* **2013**, *52*, 6606–6610. [[CrossRef](#)] [[PubMed](#)]
46. Seifert, A.; Antonovici, M.; Hauer, B.; Pleiss, J. An Efficient Route to Selective Bio-oxidation Catalysts: An Iterative Approach Comprising Modeling, Diversification, and Screening, Based on CYP102A1. *ChemBioChem* **2011**, *12*, 1346–1351. [[CrossRef](#)] [[PubMed](#)]
47. Rao, S.R.; Ravishankar, G.A. Vanilla flavour: Production by conventional and biotechnological routes. *J. Sci. Food Agric.* **2000**, *80*, 289–304.
48. Sambrook, J.; Russell, D. *Molecular Cloning: A Laboratory Manual*, 3rd ed.; Cold Spring Harbor Laboratory Press: New York, NY, USA, 2001; ISBN 978-087969577-4.
49. Maurer, S.; Urlacher, V.; Schulze, H.; Schmid, R.D. Immobilisation of P450 BM3 and an NADP<sup>+</sup> cofactor recycling system: Towards a technical application of heme-containing monooxygenases in fine chemical synthesis. *Adv. Synth. Catal.* **2003**, *345*, 802–810. [[CrossRef](#)]
50. Klaus, T. Novel Route to Vanillin—An Enzyme-Catalyzed Multi-Step Cascade Synthesis. Ph.D. Thesis, Universitaet Stuttgart, Stuttgart, Germany, 10 May 2017. [[CrossRef](#)]
51. Omura, T.; Sato, R. The Carbon Monoxide-Binding Pigment of Liver Microsomes. I. Evidence for Its Hemoprotein Nature. *J. Biol. Chem.* **1964**, *239*, 2370–2378. [[PubMed](#)]

52. Omura, T.; Sato, R. The Carbon Monoxide-Binding Pigment of Liver Microsomes. II. Solubilization, Purification, and Properties. *J. Biol. Chem.* **1964**, *239*, 2379–2385. [[PubMed](#)]
53. Bradford, M.M. A rapid and sensitive method for the quantitation of microgram quantities of protein utilizing the principle of protein-dye binding. *Anal. Biochem.* **1976**, *72*, 248–254. [[CrossRef](#)]
54. Hess, B.; Kutzner, C.; van der Spoel, D.; Lindahl, E. GROMACS 4: Algorithms For Highly Efficient, Load-Balanced, And Scalable Molecular Simulation. *J. Chem. Theory Comput.* **2008**, *4*, 435–447. [[CrossRef](#)]
55. van der Spoel, D.; Lindahl, E.; Hess, B.; Groenhof, G.; Mark, A.E.; Berendsen, H.J.C. GROMACS: Fast, Flexible, and Free. *J. Comput. Chem.* **2005**, *26*, 1701–1718. [[CrossRef](#)] [[PubMed](#)]
56. Wensink, E.J.W.; Hoffmann, A.C.; van Maaren, P.J.; van der Spoel, D. Dynamic Properties Of Water/Alcohol Mixtures Studied By Computer Simulation. *J. Chem. Phys.* **2003**, *119*, 7308–7317. [[CrossRef](#)]
57. Hoover, W.G. Canonical dynamics: Equilibrium phase-space distributions. *Phys. Rev. A* **1985**, *31*, 1695–1697. [[CrossRef](#)]
58. Nose, S. A Unified Formulation of the Constant Temperature Molecular-Dynamics Methods. *J. Chem. Phys.* **1984**, *81*, 511–519. [[CrossRef](#)]
59. Parrinello, M.; Rahman, A. Polymorphic Transitions in Single-Crystals—A New Molecular-Dynamics Method. *J. Appl. Phys.* **1981**, *52*, 7182–7190. [[CrossRef](#)]
60. Ryckaert, J.P.; Ciccotti, G.; Berendsen, H.J.C. Numerical-Integration Of Cartesian Equations Of Motion Of A System With Constraints—Molecular-Dynamics Of N-Alkanes. *J. Comput. Phys.* **1977**, *23*, 327–341. [[CrossRef](#)]
61. Essmann, U.; Perera, L.; Berkowitz, M.L.; Darden, T.; Lee, H.; Pedersen, L.G. A Smooth Particle Mesh Ewald Method. *J. Chem. Phys.* **1995**, *103*, 8577–8593. [[CrossRef](#)]
62. York, D.M.; Darden, T.A.; Pedersen, L.G. The Effect Of Long-Range Electrostatic Interactions In Simulations Of Macromolecular Crystals—A Comparison Of The Ewald And Truncated List Methods. *J. Chem. Phys.* **1993**, *99*, 8345–8348. [[CrossRef](#)]
63. DeLano, W.L. *The PyMOL Molecular Graphics System 2002*; De Lano Scientific: San Carlos, CA, USA, 2002.
64. Duan, Y.; Wu, C.; Chowdhury, S.; Lee, M.C.; Xiong, G.M.; Zhang, W.; Yang, R.; Cieplak, P.; Luo, R.; Lee, T.; et al. A point-charge force field for molecular mechanics simulations of proteins based on condensed-phase quantum mechanical calculations. *J. Comput. Chem.* **2003**, *24*, 1999–2012. [[CrossRef](#)] [[PubMed](#)]
65. Wang, J.M.; Wolf, R.M.; Caldwell, J.W.; Kollman, P.A.; Case, D.A. Development and testing of a general amber force field. *J. Comput. Chem.* **2004**, *25*, 1157–1174. [[CrossRef](#)]
66. Dupradeau, F.Y.; Pigache, A.; Zaffran, T.; Savineau, C.; Lelong, R.; Grivel, N.; Lelong, D.; Rosanski, W.; Cieplak, P. The R.E.D. tools: Advances in RESP and ESP charge derivation and force field library building. *Phys. Chem. Chem. Phys.* **2010**, *12*, 7821–7839. [[CrossRef](#)] [[PubMed](#)]
67. Frisch, M.J.; Trucks, G.W.; Schlegel, H.B.; Scuseria, G.E.; Robb, M.A.; Cheeseman, J.R.; Scalmani, G.; Barone, V.; Mennucci, B.; Petersson, G.A.; et al. *Gaussian 09, Revision B.01*; Gaussian, Inc.: Wallingford, CT, USA, 2009.
68. Berendsen, H.J.C.; Grigera, J.R.; Straatsma, T.P. The Missing Term In Effective Pair Potentials. *J. Phys. Chem.* **1987**, *91*, 6269–6271. [[CrossRef](#)]

